INTERNATIONAL JOURNAL FOR NUMERICAL METHODS IN FLUIDS, VOL. 4, 539–555 (1984)

SOLUTION OF THREE-DIMENSIONAL VISCOUS INCOMPRESSIBLE FLOWS BY A MULTI-GRID METHOD

L. FUCHS AND H.-S. ZHAO*

Department of Gasdynamics, The Royal Institute of Technology, Stockholm, Sweden

SUMMARY

The three-dimensional Navier–Stokes equations for viscous incompressible fluids are discretized on staggered or non-staggered grids. The system of finite-difference equations is solved by a multi-grid method. The method and some possible sources of difficulties and their remedies are described. The numerical algorithm has been applied to the computations of flows in ducts for a range of Reynolds numbers up to 2000. As outflow boundary conditions, either the fully developed flow profile (Dirichlet condition) or parabolic conditions have been applied. The multi-grid method has a fast rate of convergence (with both types of boundary conditions), and it is not sensitive to the number of mesh points and the Reynolds number. The numerical solution, using parabolic boundary conditions, is insensitive to the location of the outflow boundary, even for large Reynolds numbers, in contrast to the solution with Dirichlet boundary conditions.

KEY WORDS Boundary Conditions Finite-differences Multi-grid Methods Navier–Stokes

1. INTRODUCTION

The numerical solution of the three-dimensional incompressible Navier–Stokes (N–S) equations has been considered to be a difficult one. The difficulties arise because the governing equations consist of a coupled elliptic system which is not linear for non-vanishing Reynolds numbers. Numerical solutions within a reasonable computational effort could have been achieved by simplifying assumptions. For certain three-dimensional problems a global parabolization[1–4] of the flow field may be assumed. The parabolization method which has been developed[4] is based on the solution of the two-dimensional N–S equations for each time-like step. The two-dimensional N–S solver uses a multi-grid (MG) method which has been generalized to three dimensions, and this is presented here. For flows in ducts the method of parabolization is most natural since the axial flow component dominates (almost everywhere) over the transversal components. By the parabolicity assumption, the computational effort and computer memory can be reduced. On the other hand, the validity of the assumptions and the resulting accuracy of the method is poor whenever the scale of the variation in the main flow direction is not large.

The MG methods which are described here, for the solution of the full three-dimensional N–S equations, require the same order of computational effort as the parabolization method (with the two-dimensional N–S MG-solver). Furthermore, the solutions are valid throughout the flow field, provided that proper boundary conditions are imposed.

---

* Visiting scientist, permanently at the Peking Institute of Aeronautics and Astronautics, China.

0271–2091/84/060539–17$01.70

Received 29 December 1982
Revised 5 April 1983

In this work we discuss the finite-difference approximation to the governing equations on staggered (SG) and non-staggered grids (NSG). The finite differences on NSG are a combination of forward and backward differences in order to maintain the ellipticity of the system in some sense.[5] The MG solution procedure and the relaxation steps are described shortly. We discuss also a proper transfer of the dependent variables (and the interaction) among the grids, in such a way that certain integral relations are independent of the grid representation.

The flow in straight square ducts is computed for a range of Reynolds numbers (Re) up to 2000. As outflow boundary conditions, we use either a fully developed flow profile (Dirichlet conditions) or conditions which result from some scale assumptions near the outflow boundary (parabolic conditions). With Dirichlet conditions, the solution may depend on the location of the outflow boundary and the Reynolds number (Re). When Dirichlet conditions are used together with large Re, one has to place the fully developed flow boundary far away from the entrance. This can be done by stretching the co-ordinate in the main flow direction. The effects of such co-ordinate stretching on the solution and the rate of convergence are discussed. We show how a modified relaxation scheme (successive plane relaxations—SPLR) can improve the convergence for highly stretched co-ordinates. The assumptions which are used to construct the relaxation schemes are stated and the difficulties which might result from these assumptions are discussed.

The problems which are associated with the Dirichlet conditions are eliminated by applying parabolic conditions. Our computational results show that the solution is not sensitive to the location of the outflow boundary, even for the largest Re which has been tested. Furthermore, the parabolic boundary condition can be incorporated into the MG solution procedure with an efficiency similar to the MG solver with Dirichlet boundary conditions.

2. THE GOVERNING EQUATIONS

It is assumed that the steady state flow of an incompressible fluid in three space dimensions is described by the following system of equations:

$$u_{xx} + u_{yy} + u_{zz} - \mathrm{Re}\,(uu_x + vu_y + wu_z) - p_x = 0 \tag{1}$$

$$v_{xx} + v_{yy} + v_{zz} - \mathrm{Re}\,(uv_x + vv_y + wv_z) - p_y = 0 \tag{2}$$

$$w_{xx} + w_{yy} + w_{zz} - \mathrm{Re}\,(uw_x + vw_y + ww_z) - p_z = 0 \tag{3}$$

$$u_x + v_y + w_z = 0 \tag{4}$$

where u, v and w are the dimensionless velocity components in the x, y and z directions, respectively; p is the dimensionless pressure and Re is the Reynolds number.

The system of equations (1)–(4) is elliptic. It has a solution if boundary conditions are specified on all the boundaries. It is enough, for example, if the velocity vector $\mathbf{q} = (u, v, w)$ is given on all the boundaries, provided that the boundary conditions satisfy the condition that the same amount of fluid enters and leaves the domain Ω. That is

$$\mathbf{q} = \mathbf{g}(x, y, z) \text{ on } \partial\Omega \text{ (the boundary of } \Omega) \tag{5}$$

is given. By equation (4)

$$\iiint_{\Omega} \nabla \cdot \mathbf{q}\, d\Omega = \iint_{\partial\Omega} \mathbf{g} \cdot d\mathbf{s}$$

then

$$\iint_{\partial\Omega} \mathbf{g} \cdot \mathrm{d}\mathbf{s} = 0 \tag{6}$$

The system of equations (1)–(4) with the boundary condition (5) and (6) results in a solution which is determined up to an additive constant in the pressure.

The exact form of the velocity vector, at the boundaries, is not always known. An analytical expression for the velocity vector is known only in special cases (solid boundaries, at 'infinity', etc.). For channel flows, the downstream velocity vector can be written in a closed form if the outflow boundary is located at 'infinity'. ($u = v = 0$, and w is the solution of $w_{xx} + w_{yy} = C$; C is chosen so that the total mass flux into the region vanishes (6).) If the computational boundary is placed at a relatively short distance then the solution may become non-physical for large Re.

To reduce the computational domain, several authors use 'less restrictive' boundary conditions at the outflow boundary (see Reference 7 and the references there). These boundary conditions state that the flow gradients in the main flow direction vanish (Neumann conditions). Here, we assume that near the outflow boundary the w-component varies more slowly in the main flow direction than in the transverse plane. If the scale of the transverse variations is of unit length then we denote the scale of variation in the z direction by δ. It is also assumed that the transverse components u and v are smaller than w and that they can be rescaled by β. When the z co-ordinate is rescaled (locally by δ) and the rescaled transverse components are introduced into the governing equations, one obtains terms which are of different orders. When $\delta \gg 1$ and $\beta \ll 1$, by neglecting all the higher order terms, one obtains the following equations which are valid locally:

$$w_{xx} + w_{yy} - \mathrm{Re}\,(uw_x + vw_y + ww_z) - (p_m)_z = 0 \tag{7}$$

$$u_{xx} + u_{yy} - \mathrm{Re}\,(uu_x + vu_y + wu_z) - \hat{p}_x = 0 \tag{8}$$

$$v_{xx} + v_{yy} - \mathrm{Re}\,(uv_x + vv_y + wv_z) - \hat{p}_y = 0 \tag{9}$$

$$u_x + v_y + w_z = 0 \tag{10}$$

and

$$\iint w(x, y, z_i)\,\mathrm{d}x\,\mathrm{d}y = \iint w(x, y, z_o)\,\mathrm{d}x\,\mathrm{d}y \tag{11}$$

where $p(x, y, z) = p_m(z) + \hat{p}(x, y)$, and z_i and z_o are the locations of the inflow and the outflow boundaries, respectively.

The system of equations above can be applied at the outflow boundary provided that the scales assumptions are reasonable. Equations (7)–(11) are parabolic with a time-like z direction. In a recent work[10] we have compared the effect of the type of outflow boundary conditions on two-dimensional channel flows. It has been found that parabolic boundary conditions are much less sensitive than the boundary conditions of Dirichlet or Neumann types. Further, we have found that it is possible to use a simplified form of equations (7)–(11), by assuming $u = v = 0$. w, at the outflow boundary, can be computed by equation (7) if $(p_m)_z$ is given. The value of $(p_m)_z$ is adjusted, via a Newton-like method, in such a way that the resulting outflow velocity profile, w, satisfies both equations (7) and (11). Since w depends on the flow upstream of the boundary, it has to be updated during the solution

procedure. In the following, we apply at the outflow boundary the velocity vector which is computed from either the parabolic equations or the free stream (Dirichlet) conditions.

When Dirichlet conditions are used it is natural to stretch the co-ordinates in the z direction: $z = z(\zeta)$.

With such a transformation the continuity equation becomes:

$$u_x + v_y + w_\zeta / z_\zeta = 0$$

which should be written in conservation law form in order to ensure that the compatibility condition is satisfied. That is,

$$(z_\zeta u)_x + (z_\zeta v)_y + w_\zeta = 0 \tag{12}$$

gives

$$\iiint_{\Omega^1} \nabla^1 \cdot \mathbf{q}^1 \, d\Omega^1 = \iint_{\partial\Omega^1} \mathbf{q}^1 \cdot d\mathbf{s}^1$$

where

$$\mathbf{q}^1 = (z_\zeta u, z_\zeta v, w)$$
$$\nabla^1 = (\partial_x, \partial_y, \partial_\zeta)$$
$$d\Omega^1 = dx\, dy\, d\zeta$$

This conservative form should be preserved also when the equations are discretized in order to secure a solution to the system (see Section 4.2).

3. FINITE-DIFFERENCE APPROXIMATIONS

Several authors have used finite differences on staggered grids (SG) to approximate the spatial derivatives of the Navier–Stokes equations. The original method of Harlow and Welch[8] for the solution of the time dependent Navier–Stokes equations (the MAC method) uses such grids. A similar grid has been also used by Brandt and Dinar[3] for the multi-grid solution of the Stokes and the Navier–Stokes equations in two space dimensions. A finite-difference approximation on a non-staggered grid (NSG) has been used for two-dimensional problems by Fuchs.[5] In this work we have used both the SG and the NSG formulations for three-dimensional flows.

In both formulations the computational domain is subdivided into small cubes with face sizes h_x, h_y and h_ζ. The dependent variables u, v, w and p are defined at different locations on the faces and inside the basic cubes for the SG and the NSG formulations. On the NSG, all dependent variables are defined at the corners of the basic cubes, whereas on the SG each velocity component is defined at the centre of that face of the basic cube which is normal to the corresponding direction. The pressure is defined at the centre of the cube.

On the staggered grid, all the derivatives, except for the convective terms for large Reynolds numbers, are approximated by second-order accurate central differences. The resulting approximation is elliptic in some sense.[3] With the following notation:

$$\partial_x = [()_{ijl} - ()_{i-1jl}]/h_x$$
$$\partial_y = [()_{ijl} - ()_{ij-1l}]/h_y$$
$$\partial_\zeta = [()_{ijl} - ()_{ijl-1}]/h_\zeta$$
$$\partial_\bullet^2 = [()_{\bullet+1} - 2()_\bullet + ()_{\bullet-1}]/h_\bullet^2$$
$$Q = z_\zeta^2(\partial_x^2 + \partial_y^2) + \partial_\zeta^2 - \mathrm{Re}\, z_\zeta(z_\zeta u \boldsymbol{\partial}_x + z_\zeta v \boldsymbol{\partial}_y + w \boldsymbol{\partial}_\zeta)$$

and

$$a\partial_{\bullet} = \begin{cases} [()_{\bullet} - ()_{\bullet-1}]/h_{\bullet} & \text{if } a \geq 0 \\ [()_{\bullet+1} - ()_{\bullet}]/h_{\bullet} & \text{if } a < 0 \end{cases}$$

The finite-difference system can be written as:

$$L_h \Phi = R \tag{13}$$

where

$$L_h = \begin{bmatrix} Q & 0 & 0 & -\partial_x z_\zeta \\ 0 & Q & 0 & -\partial_y z_\zeta \\ 0 & 0 & Q & \partial_\zeta \\ \partial_x z_\zeta & \partial_y z_\zeta & \partial_\zeta & 0 \end{bmatrix}$$

$$\Phi = (u, v, w, p)^{\mathrm{T}} \quad \text{and} \quad R = (0, 0, 0, 0)^{\mathrm{T}}$$

The above staggered grid finite-difference equations may be interpreted as being equivalent to a finite volume formulation. The governing equations are written then in form of conservation laws and these can be satisfied on any sub-volume of the domain, and in particular for each basic computational cube. The resulting algebraic equations are exactly the same as those obtained by the SG finite-difference approximations.

On the non-staggered grid, a combination of forward and backward finite differences is used to approximate first derivatives. We introduce the following notation:

$$\partial_{\bullet}^{\mathrm{F}} = [()_{\bullet+1} - ()_{\bullet}]/h_{\bullet} \qquad \partial_{\bullet}^{\mathrm{B}} = [()_{\bullet} - ()_{\bullet-1}]/h_{\bullet}$$

$$a\partial_{\bullet} = \begin{cases} a\partial_{\bullet}^{\mathrm{B}} & \text{if } a \geq 0 \\ a\partial_{\bullet}^{\mathrm{F}} & \text{if } a < 0 \end{cases}$$

$$\partial_{\bullet}^2 = \partial_{\bullet}^{\mathrm{F}} \partial_{\bullet}^{\mathrm{B}} = \partial_{\bullet}^{\mathrm{B}} \partial_{\bullet}^{\mathrm{F}}$$

$$\nabla^2 = z_\zeta^2 (\partial_x^2 + \partial_y^2) + \partial_\zeta^2$$

$$Q = \nabla^2 - \mathrm{Re}\, z_\zeta (z_\zeta u \partial_x + z_\zeta v \partial_y + w \partial_\zeta)$$

The finite-difference approximation to equations (1)–(4) on a NSG can also be written as:

$$L_h \Phi = R \tag{14}$$

where

$$L_h = \begin{bmatrix} Q & 0 & 0 & -\partial_x^{\mathrm{F}} z_\zeta \\ 0 & Q & 0 & -\partial_y^{\mathrm{F}} z_\zeta \\ 0 & 0 & Q & -\partial_\zeta^{\mathrm{F}} \\ \partial_x^{\mathrm{B}} z_\zeta & \partial_y^{\mathrm{B}} z_\zeta & \partial_\zeta^{\mathrm{B}} & 0 \end{bmatrix}$$

$$\Phi = (u, v, w, p)^{\mathrm{T}} \quad \text{and} \quad R = (0, 0, 0, 0)^{\mathrm{T}}$$

The system of equations, as its two-dimensional counterpart,[5] is elliptic in the sense that for any (non-constant) Fourier-component of the error, the residual is non-vanishing.

It should be pointed out that interchanging the forward and backward differences in system (14) will also lead to an elliptic system, with the same (formal) first-order accuracy. Using second-order accurate central differences leads to a quasi-elliptic system,[5] for which at

least one (high-frequency) component of the error would always result in a vanishing residual independent of the amplitude of that error component. These spurious error components can be filtered out by taking some averages, but then the resulting accuracy would be still of the first order. In this work, formulation (14) is used for non-staggered grid computations.

4. THE SOLUTION PROCEDURE

The multi-grid (MG) method has been used for the fast solution of finite-difference equations. Here, we describe the basic steps and ideas of MG techniques. More details of the basic MG method for elliptic and mixed elliptic–hyperbolic equations as well as systems of equations can be found in References 2, 3 and 9. Further, we discuss several aspects of the MG method which are of importance, especially when the mesh spacing is non-uniform.

4.1. Multi-grid cycling procedure

The idea of multi-grid methods (MGM) is based upon the properties of (some standard) relaxation procedures. The error of an approximation to the solution of the finite-difference equations can be decomposed into its (finite number of) Fourier components. The shortest wavelengths (high frequencies) which can be represented on a given net are of the same order as the mesh size. Many usual relaxation methods have the property that they reduce the amplitude of the high frequency error components (which have only short range effects) while low frequencies (slowly varying global errors) are eliminated slowly. The MGM uses a sequence of grids and, usually, only one relaxation operator to eliminate efficiently a corresponding sequence of error components. The dependent variables and the equations are transferred among the grids so that the sequence of approximations may be regarded as part of the limiting procedure in approximating the differential equations by finite-difference equations.

For the MG solution procedure, of equations (13) or (14), one defines a sequence of M grids with mesh spacings $h_1, h_2, \ldots, h_M$ such that the finest grid has the spacing h_M. Usually $h_{k-1}/h_k = 2 (1 < k \leqslant M)$. The MG cycling procedure for the solution of (13) or (14), on a sequence of M grids, is as follows:

On each grid $k (1 \leqslant k \leqslant M)$ one has to solve, approximately, (i.e. to smooth out the errors of) the problem which is denoted by

$$L_k \varphi^k = R^k$$

where L_k is a finite-difference approximation to the differential operator, on a grid k; φ^k and R^k are defined below. φ^M (the current finest grid approximation) and R^M (the right-hand side on the finest grid) are given.

Then for any k the following is performed:

I. Relaxation sweeps are carried out on the grid k until the convergence is too slow.

Than either

II. The problem is transferred to a coarser grid $(k-1)$. The transfers include the dependent variables (Full Approximation Storage, FAS[2,3]) $\varphi^{k-1} = I_k^{k-1} \varphi^k$ and the residuals, such that the new right-hand side is given by:

$$R^{k-1} = L_{k-1} I_k^{k-1} \varphi^k + I_k^{k-1} (R^k - L_k \varphi^k) \tag{15}$$

where I_k^{k-1} is the transfer (interpolation or restriction operator) from the fine (k) to the

coarse grid $(k-1)$ (see Section 4.3). Step I. is repeated on the transferred problem on grid $k-1$;

or if convergence to some accuracy has been obtained, then:

III. The correction is transferred (via some interpolation) to a finer grid $(k+1)$. These corrections are smoothed out by some relaxation sweeps (step I).

The procedure ends when the prescribed accuracy is attained on the finest grid $(k=M)$.

The basic MG scheme can be a fixed one by determining, *a priori*, the number of relaxation sweeps and the sequence of transfer among the grids. The gains obtained by a more sophisticated control are marginal or none.

4.2. The relaxation procedure

The relaxation of the system (13) or (14) is done in steps. First, the three momentum equations are relaxed successively, pointwise (by a Gauss–Seidel technique). This step is straightforward and is not described here. In the second step the continuity equation is relaxed, pointwise, by changing all the dependent variables in a certain neighbourhood of each point, such that the residual of the momentum equations will remain unchanged. This can be achieved by defining a correction function χ and from it correction velocity components $\Delta\mathbf{q}=(\Delta u, \Delta v, \Delta w)$ and correction pressure, Δp, in the following manner:

$$\text{A. (SG)}\quad \Delta u = z_\xi \partial_x \chi; \qquad \Delta v = z_\xi \partial_y \chi; \qquad \Delta w = \partial_\xi \chi \qquad \Delta p = Q\chi \tag{16}$$

$$\text{B. (NSG)}\quad \Delta u = z_\xi \partial_x^F \chi; \qquad \Delta v = z_\xi \partial_y^F \chi; \qquad \Delta w = \partial_\xi^F \chi \qquad \Delta p = Q\chi \tag{17}$$

For both cases the changes in the residuals of the momentum equations can be approximated by:

$$Q\Delta\mathbf{q} - \operatorname{grad}\Delta p = 0$$

provided that

$$Q \operatorname{grad} = \operatorname{grad} Q$$

By inserting relations (16) and (17) into the respective approximation to the continuity equation, one obtains an equation for χ, i.e.

$$(x_\xi^2\partial_x^2 + z_\xi^2\partial_y^2 + \partial_\xi^2)\chi = -[(z_\xi u)_x + (z_\xi v)_y + w_\xi] \tag{18}$$

To solve equation (18) one has to specify boundary conditions on χ. From relations (16) and (17) one has to choose $\Delta u = \Delta v = \Delta w = 0$ on the boundaries. Such boundary conditions would result in a (unique) solution if and only if the right-hand side of (18) is identically zero (and the solution itself is then identically zero), or no solution would exist at all. To obtain a solution, one may specify only one condition on each boundary. This in turn means that the residuals of the momentum equations cannot be kept unchanged, at least near the boundaries, even for vanishing Reynolds numbers. By choosing a particular form of χ (non-vanishing only at a single point), Brandt and Dinar[3] constructed their distributive Gauss–Seidel (DGS) relaxation scheme. Any choice of χ which satisfies (16) or (17), and (18) is equivalent to the assumption that the approximation at each step can be corrected by a velocity flow field which is irrotational. The irrotationality assumption is most erroneous near

the boundaries where the no-slip boundary condition cannot be satisfied. It is also inaccurate when the error is strongly rotational.

Equation (18) is nothing more than the Poisson equation (and is independent of Re), and it can be relaxed efficiently by standard techniques (such as Gauss–Seidel relaxations).

The explicit and the implicit assumptions which have been adopted in this relaxation procedure can be summarized as follows:

A. The operator Q is linearized as if it had constant coefficients.
B. The Q and the grad operators are assumed to commute.
C. The correction field is assumed to be locally irrotational.

These assumptions are not always accurate enough, and the method might then diverge. Assumptions A and B are not good enough if there are large gradients in the flow field or in the error together with large Re. Assumption C is poor when the error is highly rotational. It must be emphasized that when I_k^{k-1}, in equation (15), is a fully averaging operator, then these assumptions do not cause degradation in the efficiency of the method provided that the initial error is not too large.

4.3. *Fine to coarse grid transfer*

When equation (18) is integrated (summed up) over any volume, the total mass flux out of that volume must be equal to the integral of the right-hand side of equation (18), i.e. the residual of the continuity equation. This compatibility condition must be satisfied also by the finite-difference approximations. This is the case indeed since the continuity equation is written in conservative form. If the compatibility condition is violated, no solution to (18) exists.

Equation (18) may be written, for any volume Ω on grid k, as

$$S_k = \sum_{ijl}^{k} R_{ijl}^k h_x^k h_y^k h_\zeta^k \tag{19}$$

where

$$R^k = \partial_x(z_\zeta u) + \partial_y(z_\zeta v) + \partial_\zeta w$$

When the sum is taken over the whole computational domain, S_k must vanish identically for all $1 \leqslant k \leqslant M$, in order to be compatible with the boundary conditions on the finest grid.

Figure 1 shows a basic computational cube of a coarse grid with spacings h_x^{k-1}, h_y^{k-1}, h_ζ^{k-1} and the 8 cubes of the fine grid, with spacings h_x^k, h_y^k, h_ζ^k, which describe the same region. Each velocity component (q^k) is defined at the centre of the corresponding face of each elementary cube. These velocity components are transferred from the fine grid (k) to the coarse grid ($k-1$) by an area averaging

$$q^{k-1} = \left(\sum A^k q^k\right) \Big/ A^{k-1} \tag{20}$$

where A^k and A^{k-1} are the face areas, normal to the q-component, corresponding to the cubes of the fine and coarse grids, respectively. The sum is taken over the 4 elements of the fine grid which subdivide the corresponding surface of the coarse grid.

The residual of the mass conservation equation is transferred by a volume averaging. We denote each volume element by V^k. The residuals, R^k, are transferred to the coarse grid by:

$$R^{k-1} = \left(\sum V^k R^k\right) \Big/ V^{k-1} \tag{21}$$

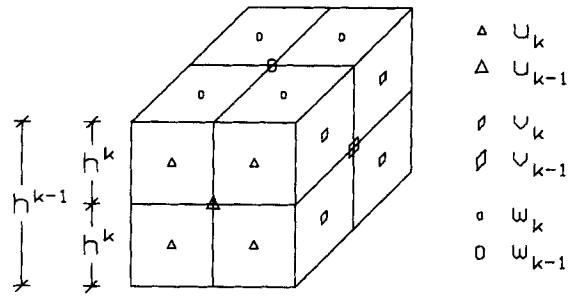

Figure 1. The transfer of the dependent variables from a grid k to a coarser grid k-1

where the sum is taken over the 8 volume elements of the fine grid which subdivide the corresponding volume element of the coarse grid. By using relations (20) and (21) one can show that the sum in equation (19) is mesh independent for any sub-domain Ω. In this way the compatibility condition is satisfied on all grids to the same accuracy as on the finest one.

The transfer of the right-hand side of the momentum equations to coarse grids may be done by an averaging similar to relation (20). This type of transfer requires more computational effort than a simpler 'injection' by which the residuals are transferred without averaging. However, an averaging often results in a faster convergence, despite the increase in computational work for each transfer, compared with injection (Section 5). This is because the averaging operator is a smoothing operator by itself in contrast to injection which may accentuate aliasing effects.

4.4. Effects of co-ordinate stretching

The use of a non-uniform mesh in the physical space requires some care in the construction of the MG solver. As already mentioned, the conservative form of the continuity equation should be used. Another important fact is that the efficiency of the relaxation operator is impaired. The MG solution procedure improves the total rate of convergence compared to other relaxation methods such as Successive Point (over) Relaxations (SPR), but the improvement depends strongly on the smoothing efficiency (of the high frequencies) of the relaxation operator. The particular choice of a relaxation operator depends on the type of problem and the range of parameters for which the solver is designed.

Under the assumptions of the previous sections, one may consider the relaxation procedure of the momentum and continuity equations as decoupled. Each step can be evaluated separately and thus one may choose an optimal relaxation operator for the given geometry. The smoothing factor of relaxation operators can be estimated by using local mode analysis.[2,3,5,6 and 9] With local mode analysis one considers the changes in the amplitudes of certain Fourier-components of the error, during the relaxation process. This analysis is valid only locally since all boundary conditions are ignored. Such an approach is most correct for high frequencies which contribute to large variations on short scales. During each relaxation step (of the momentum equations or equation (18)) an equation, with a principal part of the Laplacian, is treated. The smoothing of the Laplace equation in two space dimensions by some relaxation operators is discussed in Reference 9. It turns out that stretching of the co-ordinates deteriorates the performance of the smoothing of the SPR, whereas a properly chosen line relaxation (SLR) improves the smoothing as the mesh size ratio departs from unity. One can show (using similar principles to those in References 5 and 9) that the results for three-dimensional cases are similar. SPR is most cost-effective when the mesh-spacing

ratio is close to unity, whereas plane relaxation (SPLR), marching in the stretched co-ordinate direction, improves the smoothing as the mesh-spacing ratio departs from unity. However, when SPLR is done, one has to solve a two-dimensional problem which requires more work than the solution of a three-diagonal matrix in the SLR case. An efficient way of doing SPLR is by using an MG method for each plane during the (global) relaxation process. By such a procedure the effort for each plane relaxation sweep is equal to about 4 SPR sweeps. The convergence per relaxation sweep is improved by SPLR but the total work required might not be less compared to the theoretically less efficient SPR. On the other hand, for large mesh–Reynolds numbers combined with large errors and non-smoothing transfer to coarse grids, SPR may diverge in the MG mode whereas the SPLR works well.

It should be pointed out that the character and treatment of the momentum equations can differ from that of the continuity equation for flows which are, at least locally, of boundary layer type. One can relax the momentum equations in the natural 'time-like' (streamwise) direction. The correction problem (18) which results from the continuity equation is always elliptic, with no bias in the flow direction. Thus, if the flow-field is not too complicated, SPLR may be applied only to the relaxation of the continuity equation, whereas the momentum equations may be relaxed by an inexpensive and natural marching method such as ADI.

5. NUMERICAL RESULTS

The methods which are described above have been applied to compute the flows in straight ducts. Boundary conditions for the cases reported here are as follows: no-slip boundary conditions are applied on all the solid walls. At the inflow boundary the velocity profile is specified, whereas at the outflow boundary either Dirichlet or parabolic conditions are used.

Stretching of the co-ordinates has been done only in the main flow direction (the z direction). The transformation is defined by a single parameter ζ, namely:

$$z = \zeta + \exp(\gamma\zeta) - 1$$

The upstream boundary is at the location $z = 0$, and the downstream boundary is located at $z = \mathrm{ZEND}$. The uniform mesh case is obtained by setting $\gamma = 0$.

In Figures 2–6 we compare some flow parameters with respect to the type of downstream boundary condition (Dirichlet or parabolic) and a range of Reynolds numbers up to 2000.

In Figure 2 we consider the variation of w and its gradient w_z (in the main flow direction) for $2 \leqslant \mathrm{Re} \leqslant 2000$ with the outflow boundary located at a fixed distance ($\mathrm{ZEND} = 2$). When Dirichlet boundary conditions are applied (Figures 2(a) and (c)), a boundary-layer-like behaviour near the outflow boundary is obtained, for large Re. The numerical solutions of these problems with parabolic boundary conditions result in smooth solutions (Figures 2(b) and (d)).

In Figures 3–5 we consider the effects of the location of the outflow boundary (ZEND). From these figures the following is concluded:

A. The boundary-layer-like behaviour of the solution (with Dirichlet boundary conditions) accentuates with increasing Re.
B. The range of the solution for which a given accuracy is attained depends on the location of the outflow boundary and the given Reynolds number (with Dirichlet conditions). For large Re ($\geqslant 200$) the solution can be considered to be accurate only in the first half of the duct (Figures 4(a) and 5(a)).

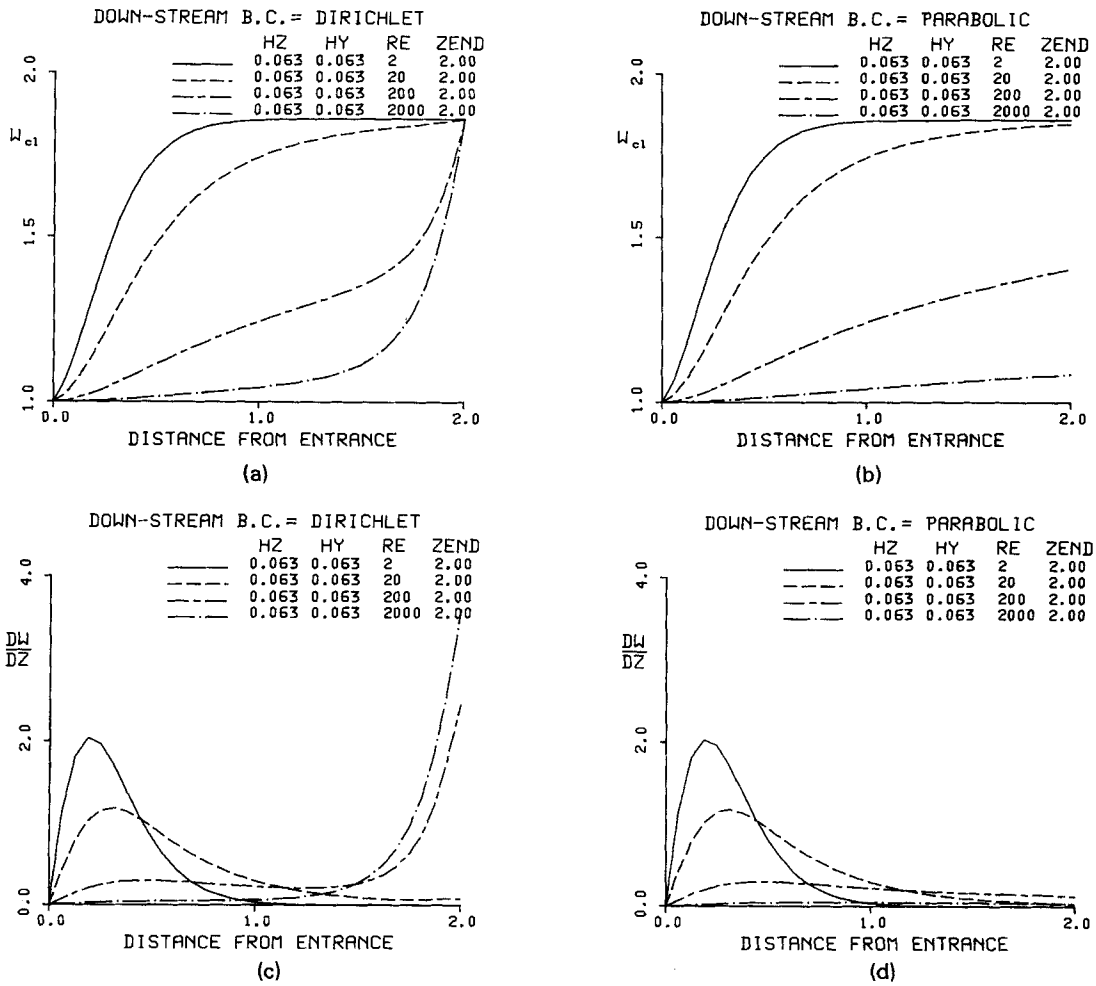

Figure 2. The variation of w and w_z along the centreline of the duct. Fixed ZEND. $2 \leqslant Re \leqslant 2000$

C. The solutions obtained with parabolic conditions applied at the outflow boundary are not sensitive to variation in ZEND for all the tested Reynolds numbers.
D. In Figures 6(a) and (b) the velocity profiles at some cross-sections are plotted, computed with Dirichlet and parabolic boundary conditions, respectively. From the plotted results it may be concluded that the solution with Dirichlet conditions converges, as ZEND increases, to the solution with parabolic conditions.

The rate of convergence of the MGM applied to SG and NSG formulations has also been studied. The transfer from fine to coarse grids is either averaged for all the equations (SG results in Table II) or averaged only for the continuity equation (NSG results in Table I). The effects of the mesh-spacing ratio, h_ζ/h ($h = h_x = h_y$), the Reynolds number and the number of the levels in the MG procedure have been considered. In all the following cases only the SPR is used, except for those which are shown in Table III.

The rate of convergence is defined to be equal to the mean reduction of the (weighted) residuals per work unit. A work unit is equivalent to the effort needed to make a single

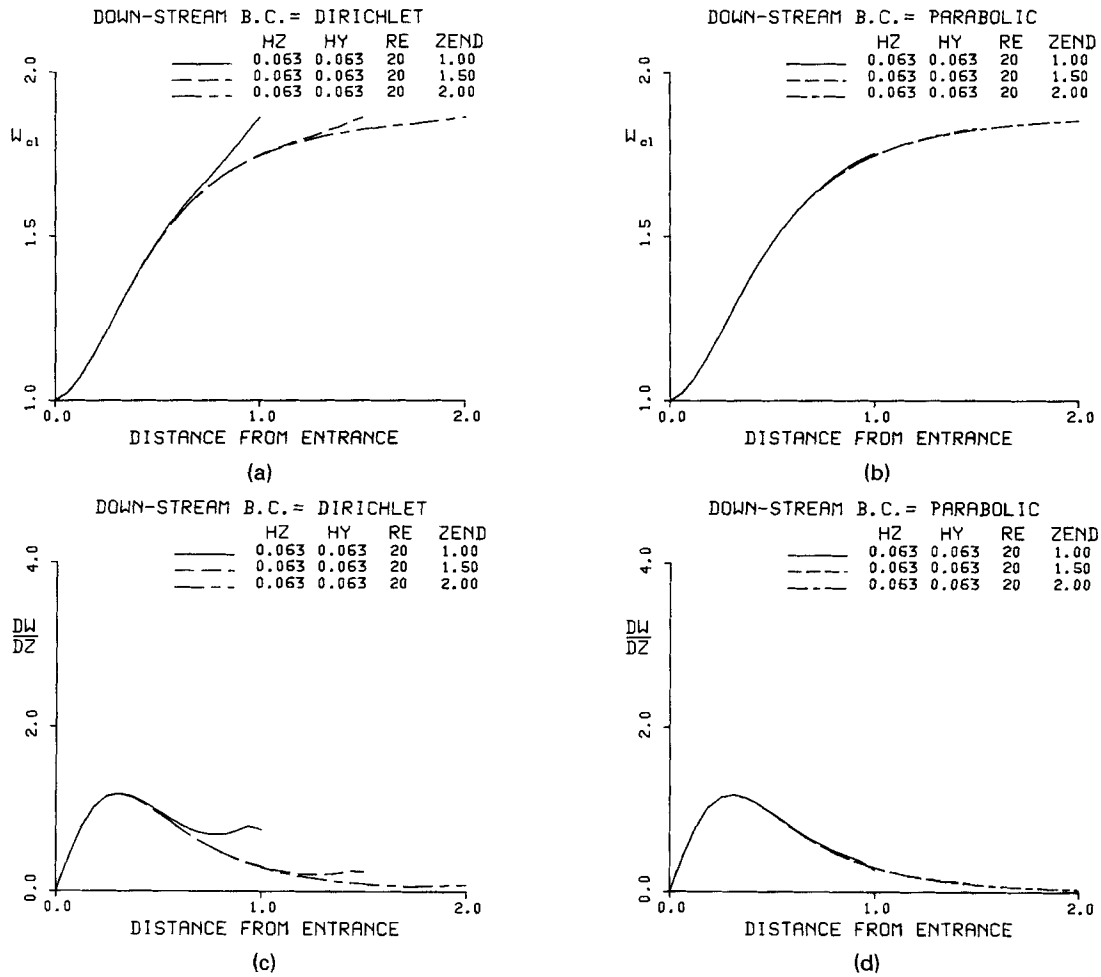

Figure 3. The variation of w and w_z along the centreline of the duct. $1{\cdot}0 \leqslant \mathrm{ZEND} \leqslant 2{\cdot}0$. $\mathrm{Re} = 20$

relaxation sweep on the finest grid. In the work-count only the relaxation effort has been taken into account, whereas the transfer among the grids has been neglected. The computations have been continued until the residuals have decreased by at least four orders of magnitude, and thus the rates of convergence in all the tables are close to the asymptotic rates of convergence of the methods. No initial approximation has been computed by coarse grid solutions.[9] For practical problems, such initial approximations may be used, and the computation is terminated at earlier stages. Under such circumstances the convergence is faster, and the (asymptotic) rates of convergence which are given here can be considered as upper bounds for practical purposes.

The sequence of grids and the number of intervals in each grid are:

A: $(4\times4\times4)$; $(8\times8\times8)$
B: $(3\times3\times3)$; $(6\times6\times6)$; $(12\times12\times12)$
C: $(6\times6\times6)$; $(12\times12\times12)$
D: $(4\times4\times4)$; $(8\times8\times8)$; $(16\times16\times16)$
E: $(8\times8\times8)$; $(16\times16\times16)$

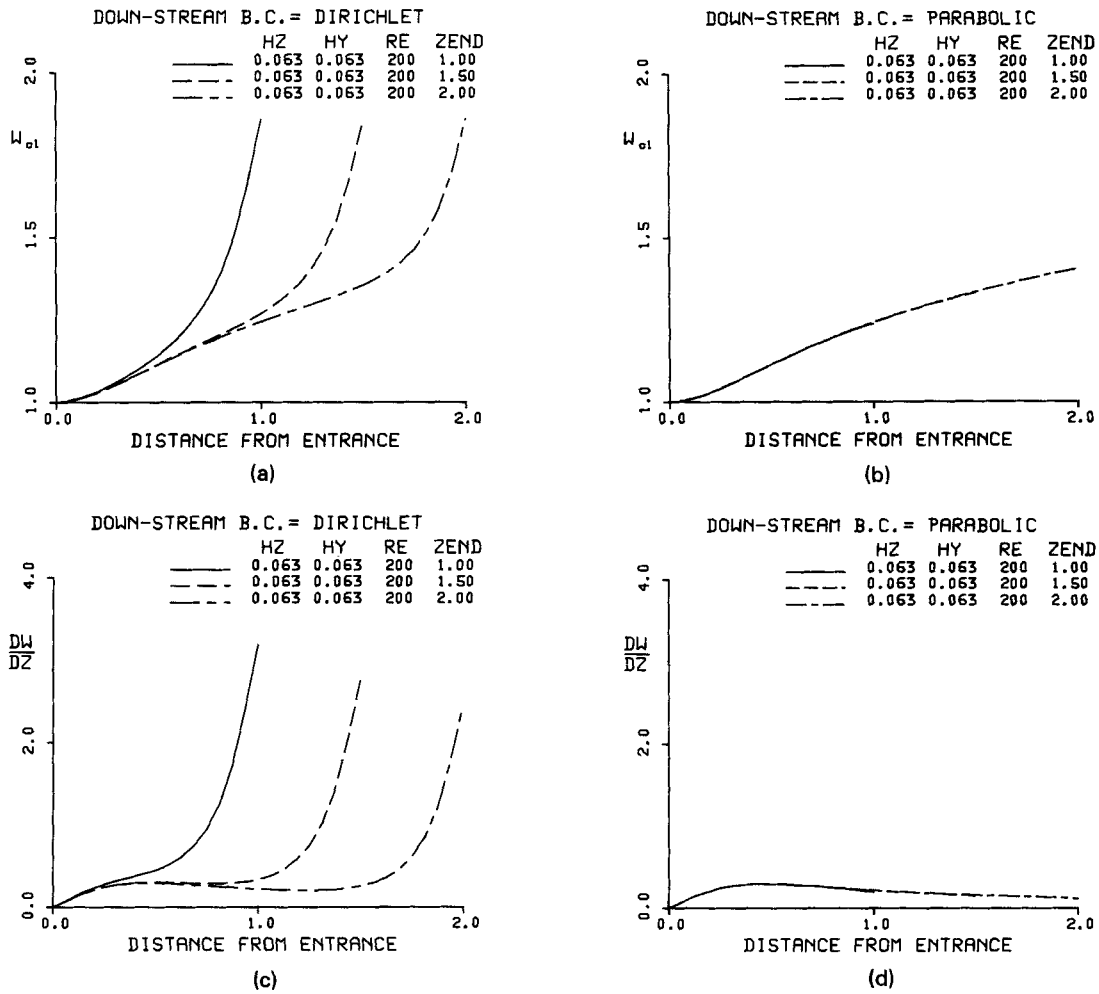

Figure 4. The variation of w and w_z along the centreline of the duct. $1{\cdot}0 \leq \mathrm{ZEND} \leq 2{\cdot}0$, $\mathrm{Re} = 200$

Table II displays the corresponding results with the SG formulation (fixed MGM with averaged transfers from fine to coarse grids)

From the tabulated results and other numerical experiments, we conclude that:

A. The SG version converges faster than the NSG version (owing to different treatment of the transfer from fine to coarse grids). However, it should be emphasized that even the NSG, with SPR, is much faster than single grid N–S solvers.

B. The rate of convergence for a given set of parameters is not sensitive to the number of points in the finest grid. This means that the computational effort is practically proportional to the number of unknowns.

C. The efficiency (with SPR) is best, for low Reynolds numbers, when the mesh-spacing ratio is close to unity. For large Re, the alignment of the relaxation direction of the momentum equations and the flow direction is important.

D. For large mesh–Reynolds numbers, $\mathrm{Re} \cdot h_\xi$, convergence is better with the fixed form of the MGM and when averaging is used for transferring residuals to coarse grids. With

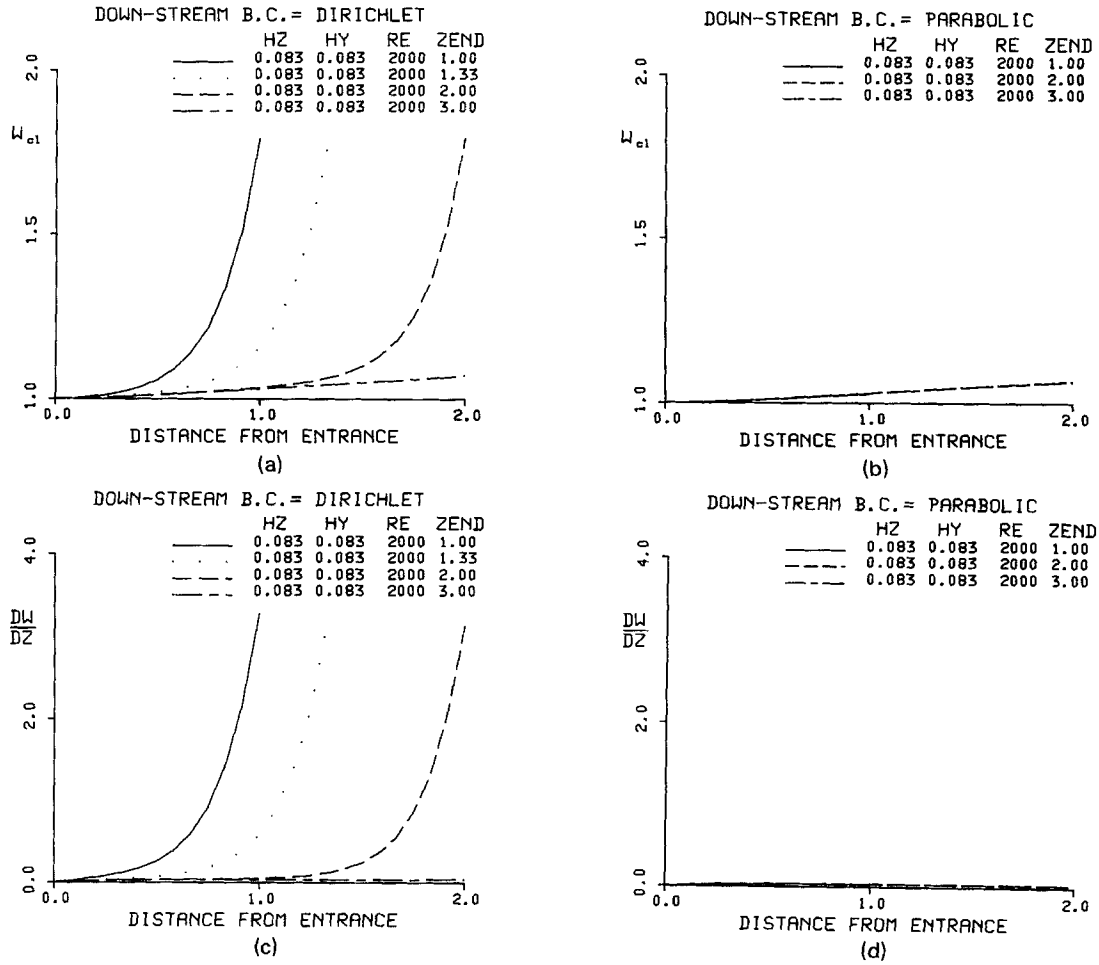

Figure 5. The variation of w and w_z along the centreline of the duct. $1{\cdot}0 \leqslant \mathrm{ZEND} \leqslant 2{\cdot}0$. $\mathrm{Re} = 2000$

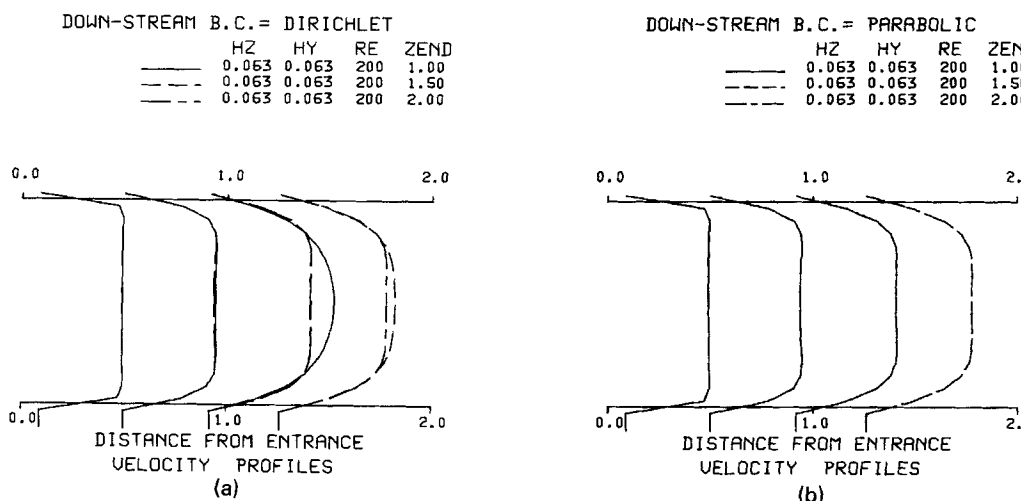

Figure 6. w velocity-component profiles at some cross-sections along the duct. $1{\cdot}0 \leqslant \mathrm{ZEND} \leqslant 2{\cdot}0$. $\mathrm{Re} = 200$

Table I. Rate of convergence of the NSG (adaptive) solver

Re	h_ξ/h	0·5	1·0	2·0	4·0
	A	0·76	0·67	0·89	—
0.	B	0·85	0·74	0·88	—
	D	0·88	0·74	0·80	—
	A	0·76	0·69	0·89	—
2.	B	0·88	0·76	0·89	—
	D	0·91	0·76	0·80	—
	A	0·78	0·78	0·84	—
20.	B	—	0·86	—	—
	C	0·81	0·78	0·85	Div
	D	0·85	0·86	—	Div
	E	—	—	0·84	—
	A	—	0·98	0·98	Div
200.	C	—	0·86	0·87	—
	E	—	0·86	0·85	—

Div = diverged.

large initial errors and large mesh–Reynolds numbers, the MG procedure may diverge. This is due to the crude linearization and the commutativity assumption between the non-linear and grad operators.

The parabolic boundary conditions have been incorporated into the SG–MGM. The main flow component has been updated in each relaxation sweep and the residuals have been transferred to coarse grids according to relation (15). The total efficiency of the MGM with parabolic boundary conditions is about the same as that with Dirichlet conditions.

Some of the results which have been obtained with SPLR are shown in Table III. The rates of convergence are based on SPLR equivalent work units which are equal to about

Table II. Rate of convergence of the SG solver

Re	h_ξ/h	0·5	1·0	2·0	4·0
	A	0·69	0·60	0·82	0·90
0.	B	0·69	0·55	0·78	0·90
	D	0·70	0·55	0·76	0·87
	A	0·59	0·58	0·80	0·91
2.	B	0·60	0·56	0·74	0·89
	D	0·65	0·57	0·73	0·92
	A	0·65	0·54	0·72	0·88
20.	B	0·65	0·54	0·70	0·86
	D	0·68	0·54	0·72	0·83
	A	0·67	0·57	0·62	0·83
200.	B	0·71	0·59	0·64	0·81
	D	0·71	0·59	0·65	0·77
	A	0·67	0·56	0·56	0·80
2000.	B	0·72	0·60	0·60	0·78
	D	0·72	0·64	0·71	0·72

The notation is the same as in Table I.

Table III. Rate of convergence of the SG solver as function of the relative mesh–Reynolds number and the mesh-spacing ratio (SPLR used)

Re	Re . h_ζ/h	h_ζ/h	Rate of convergence
25	50	2·0	0·65
	100	4·0	0·68
	200	8·0	0·80
50	25	0·5	0·65
	50	1·0	0·63
	100	2·0	0·61
	200	4·0	0·64
	400	8·0	0·71
100	50	0·5	0·71
	100	1·0	0·60
	200	2·0	0·59
	400	4·0	0·67

4 SPR work units. By using SPLR, results can be obtained, efficiently, even for large mesh–Reynolds numbers, stretching and large mesh-spacing ratios. The theoretically expected fast convergence for large mesh-spacing ratios is not attained since for large Re . h_ζ the decoupling of the relaxation of the momentum and the continuity equations is not complete.

In cases where the mesh-spacing ratio increases gradually, the SPR method converges well, even for a relatively large mesh-spacing ratio. In Table IV the rate of convergence for non-uniform NSG is shown. For Re = 20 the rate of convergence is constant for $\gamma \leqslant 1{\cdot}5$. For larger γ, for which the mesh–Reynolds numbers are above 10, the efficiency of the method decreases, and for even larger values of γ the MG procedure, without averaging the residual transfer, may diverge.

Table IV. Rate of convergence of the NSG solver as function of the stretching parameter γ (SPR used)

Re	γ	h_ζ/h	Rate of convergence
20	0·00	1·0	0·75
	0·25	1·3	0·75
	0·50	1·8	0·73
	0·75	2·5	0·74
	1·00	3·5	0·76
	1·50	6·9	0·76
	200	13·5	0·82
50	0·00	1·0	0·78
	0·25	1·3	0·76
	0·50	1·8	0·78
	1·00	3·5	0·83

6. CONCLUDING REMARKS

The MGM for the solution of the Navier–Stokes equations has been shown to be efficient and reliable. The current SG formulation converges faster than the corresponding NSG algorithm because it uses fully averaged residual transfer from fine to coarse grids. The MGM converges well with SPR, as long as the mesh-spacing ratio is not too large (and for large Re, if the initial approximation is not too bad). Large mesh-spacing ratios can be treated well by SPLR, and these are cost-effective for large ratios when SPR looses its smoothing efficiency.

The choice of boundary conditions is important and depends on the extent of the computational domain and the Reynolds number. Parabolic boundary conditions which have been incorporated into the MGM allow the reduction of the computational domain, which in turn means that the number of nodal points and mesh non-uniformities may be reduced. The methods presented here need only the same order of computational time as the globally parabolized methods. The globally parabolized methods, on the other hand, are not uniformly valid in contrast to the current three-dimensional N–S solvers.

REFERENCES

1. S. V. Patankar and D. B. Spalding, 'A calculation procedure for heat, mass and momentum transfer in three-dimensional parabolic flows', *Int. J. Heat and Mass Transfer*, **15,** 1781–1806 (1972).
2. A. Brandt, 'Multi-level adaptive solution to boundary-value problems', *Math. Comp.*, **31,** 333–390 (1977).
3. A. Brandt and N. Dinar, 'Multigrid solution to elliptic flow problems', in *Numerical Methods in PDE*, Ed. S. V. Parter, Academic Press, New York, 1977, pp. 53–147.
4. L. Fuchs and H.-S. Zhao, 'Numerical simulation of three-dimensional flows in ducts', in *Numerical Methods in Laminar and Turbulent Flow*, Eds. C. Taylor and J. W. Schrefler, Pineridge Press, 1981, pp. 167–178.
5. L. Fuchs, 'Multi-grid solution of the Navier–Stokes equations on non-uniform grids', *NASA CP-2202*, 83–100 (1981).
6. L. Fuchs, 'Finite-difference methods for plane steady inviscid transonic flows', *TRITA GAD-2* (1977).
7. P. J. Roache, *Computational Fluid Dynamics*, Hermose Publishers, 1972.
8. F. H. Harlow and J. E. Welch, 'Numerical calculation of time-dependent incompressible flow', *Phy. of Fluids*, **8,** 2182–2187 (1965).
9. L. Fuchs, 'A fast numerical method for the solution of boundary value problems', *TRITA GAD-4* (1980).
10. L. Fuchs, 'Boundary condition effects on the computation of channel flows', *Proc. Second Asian Congress of Fluid Mechanics* (1983).